Postprint of: Błażek K., Kasprzyk P., Datta J., Diamine derivatives of dimerized fatty acids and bio-based polyether polyol as sustainable platforms for the synthesis of non-isocyanate polyurethanes, Polymer, Vol. 205 (2020), 122768, DOI: 10.1016/j.polymer.2020.122768

Diamine derivatives of dimerized fatty acids and bio-based polyether polyol as sustainable platforms for the synthesis of non-isocyanate polyurethanes

Kamila Błażek[1], Paulina Kasprzyk[1], Janusz Datta*[1]

[1]Gdansk University of Technology, Faculty of Chemistry, Department of Polymers Technology, 11/12 Gabriela Narutowicza Street, 80-233 Gdansk, Poland
*Corresponding author e-mail address: janusz.datta@pg.edu.pl

ABSTRACT

A series of environmentally friendly non-isocyanate polyurethanes (NIPUs) were successfully prepared via the polyaddition reaction of bio-based polyether polyol-based cyclic carbonate with diamine derivative of dimerized fatty acids. The syntheses of NIPUs were realized by the three-step method in the absence of toxic solvents and, importantly, the process of carbonation did not require the use of elevated pressure. The effect of using various types of bio-based amines, [amine]/[cyclic carbonate] molar ratio as well as different reaction temperatures on the chemical structure and thermal properties were widely investigated by Fourier transform infrared spectroscopy (FTIR), differential scanning calorimetry (DSC), and thermogravimetric analysis (TGA), respectively. The Gaussian deconvolution technique was used to decompose the carbonyl region (-C=O) of three peaks in various samples. It was found that the molar ratio of substrates and curing temperature have an effect on the distribution of free and H-bonded carbonyl groups as well as carbonyl groups from cyclic carbonates in the chemical structure of the prepared compounds. On this basis, the role of hydrogen bonds in the chemical structure of NIPU on selected sample properties was determined. Moreover, the impact of water during 6 months of immersion on the polymer networks was examined.

Keywords: non-isocyanate polyurethanes; carbon dioxide; bio-based substrates

1. Introduction

Polyurethanes (PUs) are among the most common and highly versatile classes of polymeric materials. Conventional polyurethane synthesis involves the use of isocyanates, ether- or ester-based polymeric diols and low-molecular-weight chain extenders (such as glycols) [1]. Environmental impacts of materials are dependent on their toxicity during the synthesis of the substrates, polymerization reaction and at the end of their life [2]. On a technical scale, the synthesis of isocyanates requires the use of phosgene, which is an extremely toxic, lethal and an energy-intensive gas. In this method, large amounts of hydrochloric acid are produced as a side product [3]. Another aspect concerns the high reactivity of a functional isocyanate group with bases, acids, amines or alcohols. A crucial aspect is a susceptibility to hydrolysis, which is the main process affecting bioaccumulation potential and the overall fate in the environment. Given the toxicity of isocyanate, exposure to even the low concentrations could pose danger for human health and consequently lead to contact dermatitis, respiratory tract disorders, respiratory sensitization, and even cancer [4]**.** Due to the growing ecological trend in chemistry, extensive efforts have been made to study the possibility of withdrawal from the use of isocyanate compounds and search for an alternative method producing PUs by isocyanate-free routs. Non-isocyanate polyurethanes (NIPUs) can be obtained by various synthetic pathways. Scientific investigations consider step-growth polyaddition, polycondensation methods, ring-opening polymerization and rearrangement reactions [5,6]. Polyaddition of bifunctional cyclic carbonates with di- or polyamines yielding poly(hydroxy urethanes)s (PHUs) seems to be the best possible synthesis route. The advantages of this method include the removal of using organic solvents and catalysts, possibility of utilization of carbon dioxide (CO_2) and use of bio-based resources. Replacing petroleum-derived chemicals by monomers obtained from green resources should give both socio-economic and environmental benefits in the long term in particular improvement of economic stability for the countries with lack of fossil fuels as well as reduction of energy consumption and greenhouse gases (especially CO_2) emission [7,8]. Cárre et al. [9] defined three classes of compounds according to the used feedstock, which are suitable for a sustainable way of synthesizing non-isocyanate polyurethanes from the perspective of green chemistry. The first group includes vegetable fats and oils. In this group, the greatest attention is paid to the carbonation reaction of epoxidized vegetable oils, the use of dimerized fatty acids as well as glycerol and its derivatives [10]. The second class is compounds derived from starch and sugar resources. This group includes such promising compounds dedicated to the bio-based NIPU synthesis as: isosorbide (ISO) [11], sorbitol (SOR) [12],

2,5-furandicarboxylic acid (FDCA) and erythritol [13]. The last group are bioresources from wood. In this group, the following compounds have been used in the NIPU synthesis: lignin [14], tannins [15], vanillin and its derivatives [16], cardanol [17], terpenes (especially limonene)[18]. It can be seen that the selection of compounds that have a high potential for use in the synthesis of bio-based NIPU is very wide, which opens up many new possibilities in agreement with the concept of sustainable development.

Our recent studies [19,20] have focused on the poly(ether-urethane-urea)s and poly(ester-urethane-urea)s synthesized via traditional method using a diamine derivative of dimerized fatty acids (Priamine® 1071) as a curing agent. This research work has been carried out in order to obtain NIPUs via the polyaddition reaction. The raw materials used for the production of PUs by the proposed method are polyether polyol-based cyclic carbonates and diamines obtained from fatty acid dimers. The first of these is made on an industrial scale by fermentation of glucose obtained from corn crops with the aid of *Escherichia coli* to receive 1,3-propanediol. A step after that is polycondensation of bio-based 1,3-propanediol (PDO). The great merits of this method are to consume 40% less energy and reduce by more than 40% greenhouse gas emissions in comparison to technology based on fossil fuel [21]. Vegetable oils composed of different triglycerides and their derivatives (e.g. fatty acid dimers) are also a promising raw material used in polymer synthesis, especially PUs. Applying dimerized fatty acids allow for receiving compounds with α,ω functionalities [22]. Priamine® provided by Croda company and used in this study is a dimer diamine functional building block with 100% renewable carbon. Dimerization of fatty acids can lead to cyclic, acyclic and aromatic structures with different composition of mono-, di- and trimers, which may affect selected properties of the finished material, crosslinking and macromolecular architectures [23].

In this work, we have synthesized NIPUs using four types of diamine derivatives of dimerized fatty acids and novel polyether polyol-based cyclic carbonate. We also examined the effect of crosslinking temperature as well as [amine]/[cyclic carbonate] molar ratio on the selected properties of the obtained materials. In order to evaluate the real potential of novel NIPUs, a comparative study of the chemical structure (by spectroscopic techniques) and thermal properties (by DSC and TGA methods) of the prepared materials was performed. Moreover, the gel content and swelling index were estimated through swelling properties in THF as a solvent. In this study, the effect of time immersing in water to the swelling ratio of prepared samples was also examined.

2. Materials and methods

2.1.Materials

The syntheses of diglycidyl ethers were carried out using commercially available bio-based poly(trimethylene glycol) (PO3G) as a bio-based platform chemical, known as Sensatis® (molecular weight: 250 g/mol), purchased from Allessa (Germany) and used as received. Epichlorohydrin (ECH) (purity ca. ≥ 99 %; molecular weight: 92.52 g/mol) as a building block, sodium hydroxide (NaOH) as dehydrochlorination agent and boron trifluoride-diethyl ether complex ($BF_3 \cdot Et_2O$) (purity ca. ≥ 98 %; molecular weight: 141.93 g/mol) as a catalyst were acquired from Sigma-Aldrich (USA) and used as received. Tetrabutylammonium bromide (TBAB) (molecular weight: 322.38 g/mol; revealed purity ca. 99 %) was purchased from TCI Chemicals (Belgium) and applied as a catalyst for the cycloaddition of carbon dioxide (CO_2). In the last step, non-isocyanate polyurethanes were prepared using bio-based diamines derivative of dimerized fatty acids Priamine® 1071, 1073, 1074 and 1075 as curing agents, purchased from Croda (Netherlands). Some of the properties of these compounds are summarized in **Table 1**. For the analytical measurement methods, all chemicals and solvents were of analytical grade and were used as received.

Table 1 Selected properties of amines used for synthesis

	Theoretical amine value [mgKOH/g]	Amine value [mgKOH/g]	M_n [g/mol]	Dimer content [wt%]	Trimer content [wt%]
Priamine 1071	205	192.9±2.1	581.9±6.3	75	25
Priamine 1073	200-210	191.2±2.0	587.0±6.1	n/a	n/a
Priamine 1074	205	203.9±0.4	550.2±1.0	n/a	n/a
Priamine 1075	205	201.6±1.1	556.5±3.1	>99	<1

Theoretical amine value was given by the manufacturer; M_n was calculated according to experimental amine value; the method of determining amine value is given in Section 2.3.2; dimer/trimer content adopted from [23]

2.2. General procedure for synthesis of non-isocyanate polyurethanes (NIPUs)

The syntheses of NIPUs were realized by the three-step method. Firstly, polyether polyol-based diglycidyl ether was synthesized through a reaction between poly(trimethylene glycol) and epichlorohydrin (see **Figure 1**) in the presence of aqueous sodium hydroxide (concentration of a solution was 50%) as a dehydrochlorination agent and 1 wt% of $BF_3 \cdot Et_2O$ as a catalyst. The synthesis was carried out in a 0.5 L glass reactor equipped with Liebig condenser, temperature controller and anchor stirrer. Firstly, 125 g of dehydrated polyol (0.5 mol) and the catalyst

(1 wt%) were added into the reactor and were heated to 80°C. After the temperature had been stabilized, 138.78 g of ECH (1.5 mol) was dosed in portions under continuous stirring. After ECH had been added, the process took *ca* 8h under continuous stirring and temperature control. Subsequently, the reaction mixture was cooled to 50 °C than 60 g of NaOH (1.5 mol) in 50% (w/w) aqueous solution was added gradually. The process took *ca* 5h. The filtration at reduced pressure was used to separate the solid precipitate from the liquid components. The extraction of the main product was realized using ethyl acetate. Finally, the solvent and unreacted substrates were evaporated. The quantitative yield of diglycidyl ether reached 94% when the molar ratio of ECH to PO3G was 3:1. In this type of reaction halohydrin ether as a side-product may be formed [24].

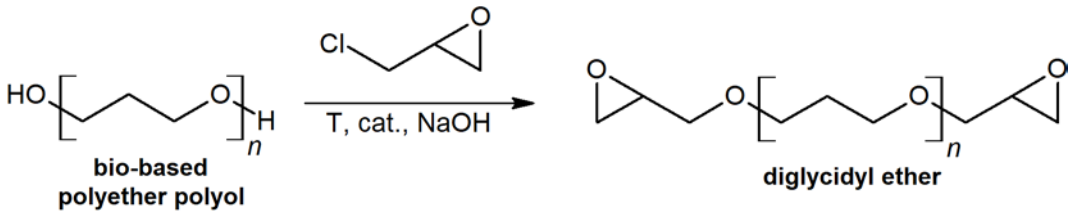

Figure 1 Synthesis of diglicydyl ether of bio-based polyether polyol (ED)

In the next step (see **Figure 2**), obtained diglycidyl ether was reacted with carbon dioxide gas without using the organic solvents in the presence of TBAB (0.5 wt%) as a catalyst. The synthesis was carried out in a 0.5 L three-necked flask (standard 14/23 and 29/32 joints) equipped with temperature controller, magnetic stirrer and equipment needed to bubble gas through the liquid. The reaction was conducted at 110 °C for 30 h under atmospheric pressure with a controlled gas flow rate (100 ml min^{-1}) measured by mass flow meter [21]. The process took *ca* 30h. The obtained five-membered bis(cyclic carbonate) could be used without any purification. The quantitative yield of cyclic carbonate reached 90%.

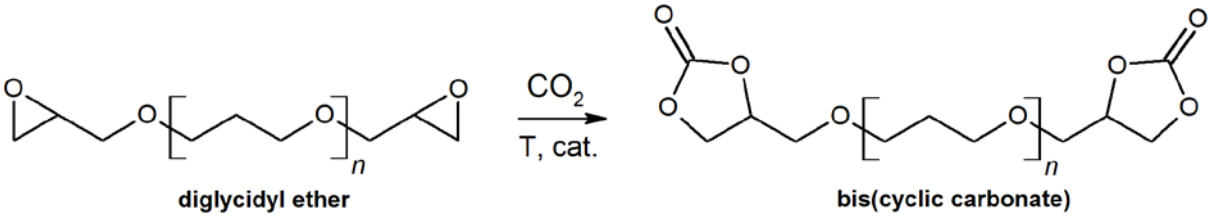

Figure 2 Synthesis of bis(cyclic five-membered carbonate) (DC) using diglicydyl ether of bio-based polyether polyol and carbon dioxide

In the last step, one-pot polymerization process between bio-based polyether polyol-based cyclic carbonates and diamine derivatives of dimerized fatty acids (Priamine® 1071, 1073, 1074

and 1075) was performed, as depicted in **Figure 3**. The mixture was mechanically stirred 3h at a temperature of 110 °C. Next, the prepared samples were cured at 100, 110, 120 and 130 °C for 48 h in a laboratory oven, which permitted to complete the reaction between cyclic carbonate and amine groups. Different NIPUs were obtained based on the variable [amine]/[cyclic carbonate] molar ratio during the reaction equal 0.8, 0.9, 1.0, 1.05, 1.1, 1.2. The size exclusion chromatography was used to characterize the number average molecular weight (M_n) of the synthesized cyclic carbonate. The M_n of DC equals 544 g mol^{-1}. The molecular mass of diamine derivatives of dimerized fatty acids was determined based on experimental amine titration (see **Table 1**).

In **Table 2**, the analyzed samples along with their classification, curing temperature as well as the content of bio-based sources are reported. The total content of bio-based components (i.e. bio-based polyols and bio-based diamines) in the structure of produced materials (NIPUs) is above 91.0%.

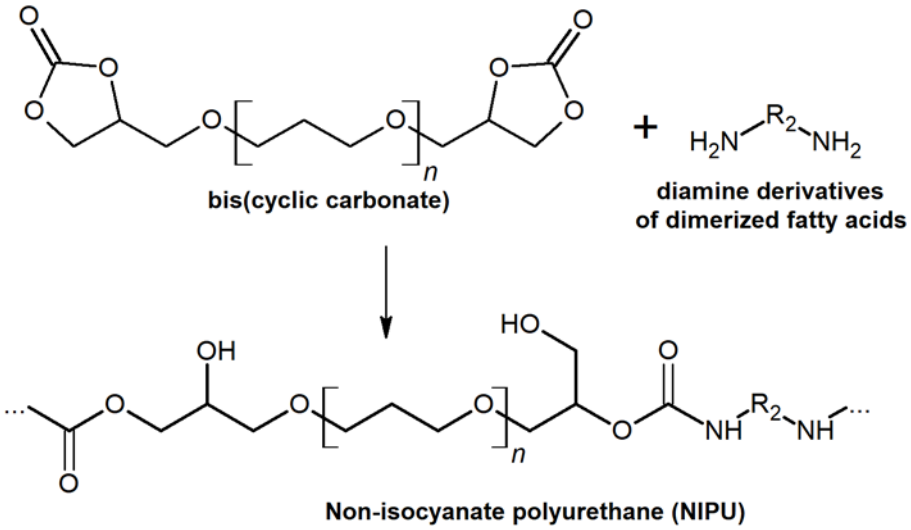

Figure 3 Synthesis of NIPUs using five-membered bis(cyclic carbonate) and diamine derivatives of dimerized fatty acids (Priamine®)

Table 2 The formulation design of bio-based NIPUs samples

Bio-based NIPU	Amine type	Amine/Cyclic carbonate molar ratio	Curing temperature [°C]	Content of bio-based sources [wt.%]*
NIPU0.8	Priamine 1071	0.8	110	91.0
NIPU0.9	Priamine 1071	0.9	110	91.6
NIPU1.0	Priamine 1071	1.0	110	92.0
NIPU1.05	Priamine 1071	1.05	110	92.3

NIPU1.1	Priamine 1071	1.1	110	92.5
NIPU1.2	Priamine 1071	1.2	110	92.9
NIPU1071	Priamine 1071	1.2	110	92.9
NIPU1073	Priamine 1073	1.2	110	92.9
NIPU1074	Priamine 1074	1.2	110	92.6
NIPU1075	Priamine 1075	1.2	110	92.7
NIPU100	Priamine 1071	1.2	100	92.9
NIPU110	Priamine 1071	1.2	110	92.9
NIPU120	Priamine 1071	1.2	120	92.9
NIPU130	Priamine 1071	1.2	130	92.9

*Content of bio-based sources is defined as the ratio of the mass of bio-based components to the total mass of the material [25].

2.3. Characterization methods

2.3.1. Epoxy number (L_E)

The epoxy number was determined by using a standard titration method, in accordance with Polish standard PN-87/C-89085/13. About 0.5 g of sample was dissolved in 15 cm^3 of hydrogen chloride–dioxane solution (2.0 mol dm^{-3}) at room temperature. Next, the mixture was titrated with a standard solution of sodium hydroxide (0.2 M ethanolic sodium hydroxide solution) with cresol red as indicator. Each analysis was repeated at least three times, and the reported results are averages of all conducted measurements per sample. The epoxy number was calculated by using the following formula:

$$L_E = \frac{(V_1 - V_2)C}{10m}, \quad (1)$$

where V_1- the volume of NaOH used during blank feed titration (cm^3); V_2- the volume of NaOH used during sample titration (cm^3); C- the molar concentration of NaOH (g mol^{-1}); m- the mass of sample (g).

2.3.2. Amine value (L_A)

The amine value of each diamine derivative of dimerized fatty acids was determined by using a standard titration method, in accordance with BN-96 6110-29. A known amount of sample (around 0.5g) was dissolved in 20 cm^3 of propan-2-ol and 5 cm^3 of water. After the dissolution was completed, five drops of bromocresol green indicator were added. The titration was made with standard 0.2 N hydrochloric acid solution to a definite yellow color. The following formula was used to calculate the amine value:

$$L_A = \frac{(V_1 - V_0)\cdot 56.1 \cdot C}{m}, \quad (2)$$

where V_1- the volume of HCl used during sample titration (cm^3); V_0- the volume of HCl used during blank feed titration (cm^3); C- the molar concentration of HCl (g mol^{-1}); m- the mass of sample (g).

The equivalent weight of used amines was calculated based on the obtained values of amine number by using the following formula:

$$E_W = \frac{56.1 \cdot 1000 \cdot f}{L_A}, \quad (3)$$

where L_A- the amine value (mol g^{-1}); f- the functionality of the compound, assumed f=2.

2.3.3. Fourier Transform Infrared Spectroscopy (ATR-FTIR)

The presence of characteristic chemical groups in the chemical structure was confirmed by means of a Nicolet 8700 FTIR Spectrophotometer (Thermo Electron Corporation, USA) and the ATR technique (Heated Golden Gate from Specac Ltd.). The spectra were acquired at room temperature using 64 scans in the wavenumber range from 4500 to 500 cm^{-1}, with a resolution of 4 cm^{-1}. In order to calculate the number of hydrogen bonded carbonyl groups, free (non-hydrogen bonded) carbonyl groups and carbonyl groups from unreacted cyclic carbonates, the deconvolution of the carbonyl peaks in the wavenumber range from 1500 to 1850 cm^{-1} was carried out using Origin software [26].

2.3.4. Nuclear magnetic resonance (^{1}H NMR)

Chemical structure of used substrates and by-products was investigated by Hydrogen Nuclear Magnetic Resonance Spectroscopy (^{1}H NMR). Spectra were recorded at the room temperature using a Varian Mercury Vx spectrometer operating at frequency of 400 MHz, by applying DMSO-d_6 as a solvent.

2.3.5. Carbonate equivalent weight (CEW) by ^{1}H NMR

The carbonate equivalent weight was determined by ^{1}H NMR spectroscopy using the procedure published by Cornille et al.[27,28]. An appropriate amount of cyclic carbonate (around 30 mg) and a standard solution of toluene with DMSO-d_6 (around 65 mg of toluene dissolved in 10 mg of DMSO-d_6) was drawn up into an NMR tube. Three characteristic cyclic carbonate peaks at 4.94, 4.53 and 4.26 ppm as well as peak located at 2.32 ppm assigned to the CH_3 of toluene were integrated.

The following formula (1) was selected to calculate the carbonate equivalent weight of the obtained bis(cyclic carbonate):

$$\textit{Carbonate equivalent weight [g/eq]} = \frac{m_{C5}}{n_{function\ of\ carbonate}} = \frac{m_{C5} \cdot I_t}{(I_a+I_b+I_c) \cdot n_t}, \quad (1)$$

where m_{C5}- mass of cyclic carbonate; $n_{function\ of\ carbonate}$- molar amount of function carbonate in cyclic carbonate; I_t- integration of peak CH_3 of toluen; I_a, I_b, I_c- integration of peaks of three cyclic carbonate protons; n_t- molar amount of toluene introduced in standard solution.

2.3.6. Thermal analysis (TGA)

Thermogravimetric Analysis was realized using NETZSCH TG 209 F3 Tarsus® Thermogravimetric Analyzer. The samples (ca. 10 mg) were placed in corundum crucible and heated from 30 to 600 ^oC with a heating rate of 20 $^oC\ min^{-1}$. The measurements were performed under a continuous nitrogen atmosphere (N_2).

2.3.7. Differential Scanning Calorimetry (DSC)

Differential Scanning Calorimetry analysis was carried out using a DSC 204 F1 Phoenix Analyzer. Firstly, the sample was heated at a rate of 20 $^oC\ min^{-1}$ from -80 to 200 ^oC. In this cycle, the thermal history of the sample was erased. Next, the sample was cooled down to -80 ^oC. The second cycle was also realized at a rate of 20 $^oC\ min^{-1}$ from -80 to 200 ^oC. The measurements were performed under a continuous nitrogen atmosphere (N_2).

2.3.8. Swelling index and gel content

The rectangular specimens was immersed in tetrahydrofuran (THF) as a solvent. The measurement was carried out at room temperature for 24 h of sample exposure to the liquid. The samples were blotted with filter paper to eliminate excess of solution and weighted.
The swelling index was calculated using the following formula (3):

$$\textit{Swelling Index}\ [\%] = \frac{Ws-Wo}{Wo} \text{ x } 100\%, \quad (3)$$

where W_o and W_s is the initial weight of sample [g] and mass after swelling, respectively.
After the swelling index measurement, samples are dried in an oven at 50 oC during 24h. The gel content was determined according to the following equation (4):

$$\textit{Gel content [\%]} = \frac{Wg}{Wo} \text{ x } 100\%, \quad (3)$$

where W_g is the weight of sample [g] after drying.

2.3.9. Determination of water absorption

The interactions of obtained materials with distilled water were studied by the standard procedure. Six samples of each materials were prepared for the water absorption evaluation. The specimens were ca. 10 mm in width, ca. 10 mm in length and ca. 2 mm in height. Test was conducted by submerging the specimens in distilled water for half a year at room temperature. The increase in weight was measured as compared to the original weight of the sample. Mass change was examined after 1, 2, 3, 7, 14, 21 days and 2 and 6 months. Water absorption was determined using the following formula (4):

$$\textit{Water absorption}\ [\%] = \frac{Wt - Wo}{Wo} \times 100\%, \quad (4)$$

where Wt- the weight of sample after 1, 2, 3, 7 days and 1, 2, 3 and 6 months of immersion in water [g]; Wo- the weight of sample before the test [g].

3. Results and discussion

A study was conducted to investigate the real potential of using synthesized polyol-based bis(cyclic five-membered carbonate) in the synthesis of novel isocyanate-free PUs. The first step of this work consisted in the preparation of diglycidyl ether by the reaction of bio-based polyether polyol from renewable resources (M_w= 250 g/mol) and epichlorohydrin. The second stage involved catalytic fixation of CO_2 into epoxy groups. On the basis of our recent studies [21], the optimum gas flow rate equals 100 ml min^{-1}. Formation of the cyclic carbonate groups was monitored by determination of the epoxy equivalent. Epoxy equivalent diminished from 0.314 ±0.012 to 0.003 ±0.002 mol of epoxy groups per 100 g of intermediate product. The percent yield of the carbonation reaction calculated on the basis of epoxy equivalent was 98.91%.

Chemical structure analysis

The structure analysis of pure components (polyol and diamines) as well as obtained intermediates (diglycidyl ether and cyclic carbonate) was performed by means of ATR-FTIR and ^{1}H NMR spectroscopy, as depicted in **Figure 4**, **Figure 5** (spectra of diamines) and **Figure 6** (spectra of polyol and intermediates).

The registered FTIR spectra (**Figure 4**) of different Priamine products are very similar. The presence of typical chemical groups in the chemical structure of diamines were confirmed. The bands related to stretching vibrations of amine groups were observed (νN-H). Bio-based

diamines are functional derivatives of fatty acids resulting from the dimerization process. Flexible long aliphatic main and side chains impact on C-H stretching, bending and rocking vibrations signals intensity. In the case of Priamine 1071, 1073, 1074, a weak absorption signal at about 900 cm^{-1} is associated with the occurrence of an aromatic ring in the chemical structure, however, this peak is really insignificant with respect to the others, which confirms their negligible amount in the chemical structure. The signal is not visible for Priamine 1075. Priamine products are prepared from linoleic and/or oleic acid and mainly displays a branched and saturated acyclic and cycloaliphatic structures [29]. The formation of bicyclic and aromatic dimer acid structures depends on the reaction conditions and used feedstock [30].

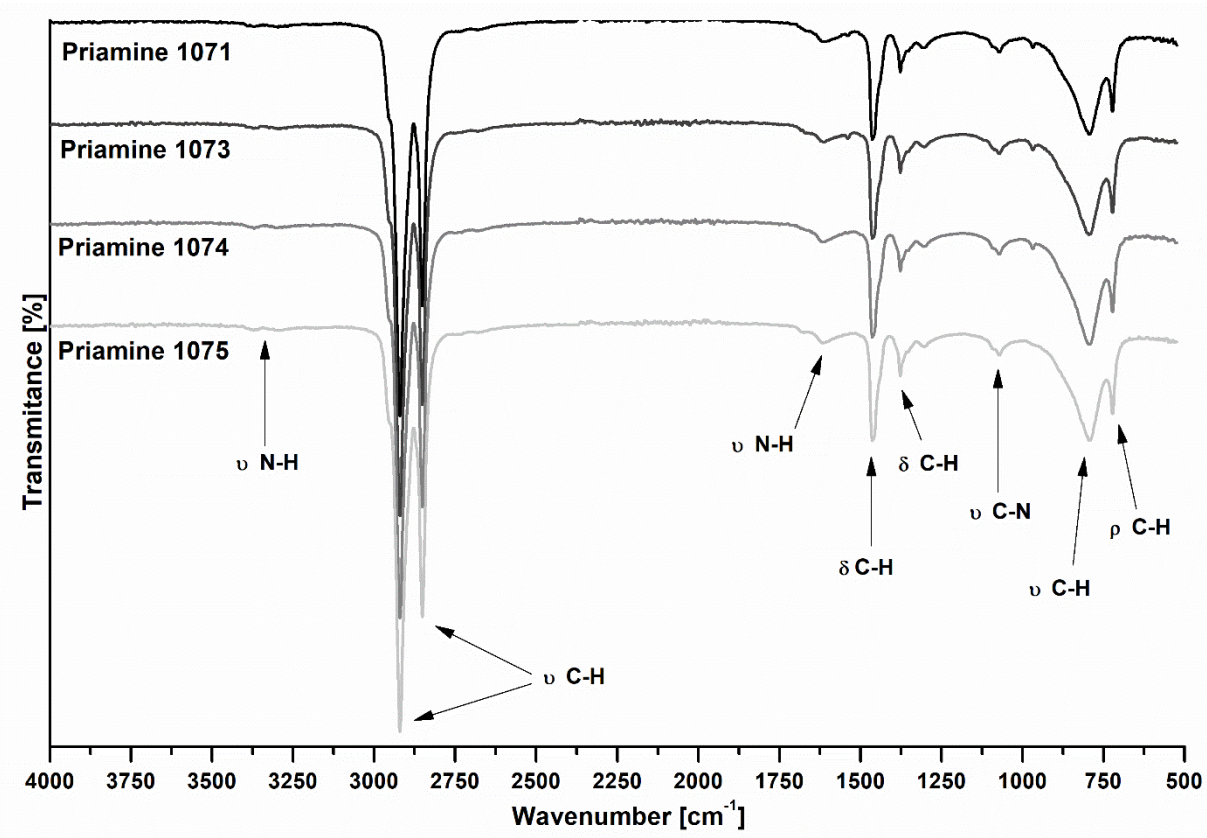

Figure 4 FTIR spectra of the diamine derivatives of dimerized fatty acids (Priamine 1071, 1073, 1074 and 1075)

Slight differences in the intensity of signals were observed in ^{1}H NMR spectra between 7.0 and 5.0 ppm in the aromatic and vinylic region (see **Figure 5**). Observed signals are attributable to the protons in -CH=CH- and -CH_2-HC=CH-CH_2- units [19]. This confirms that in the chemical structure of the mentioned amine derivative of dimerized fatty acids aliphatic and cyclic structures as well as a small amount of aromatic structures are presented.

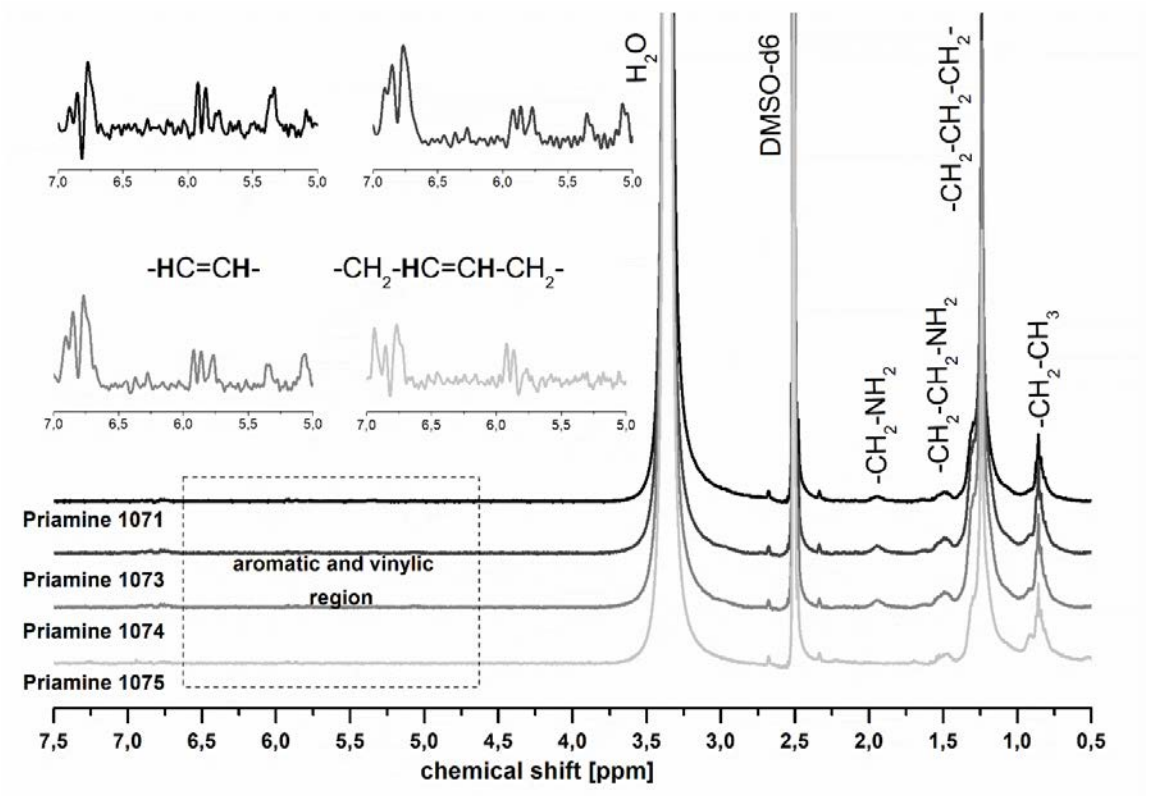

Figure 5 ^{1}H NMR spectra of bio-based diamines Priamine 1071, 1073, 1074 and 1075

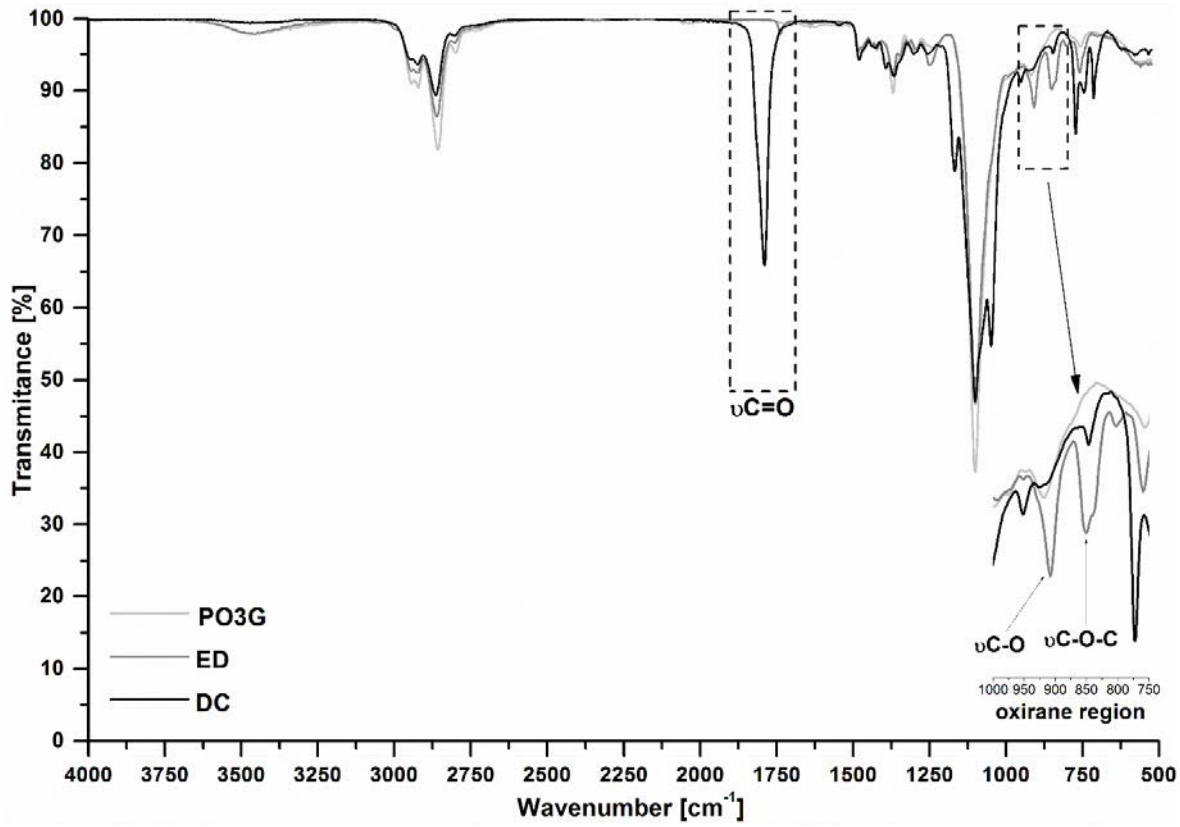

Figure 6 FTIR spectra of the original bio-based polyether polyol, diglycidyl ether and bis(cyclic five-membered carbonate) (**Appendix S1**- color version of Figure 6)

The structures of the commercial bio-based polyol, obtained diglycidyl ether and cyclic carbonate were determined by ATR-FTIR spectroscopy (see **Figure 6**). We were expected modification of hydroxyl groups into epoxide end groups. Subsequent reaction with CO_2 has converted these groups into cyclic carbonate moieties. In the registered spectrum of diglycidyl ether, the bands indicating the presence of the oxirane groups in the backbone at 846 cm^{-1} (νC-O-C) and 908 cm^{-1} (νC-O) were observed. These characteristic bands has been disappearing gradually during incorporation of CO_2. At the same time, the gradual formation of the distinctive absorption peak at 1800 cm^{-1} assigned to the C=O stretching vibrations in cyclic carbonate groups were registered in the FTIR spectrum and confirmed the formation of cyclic carbonate.

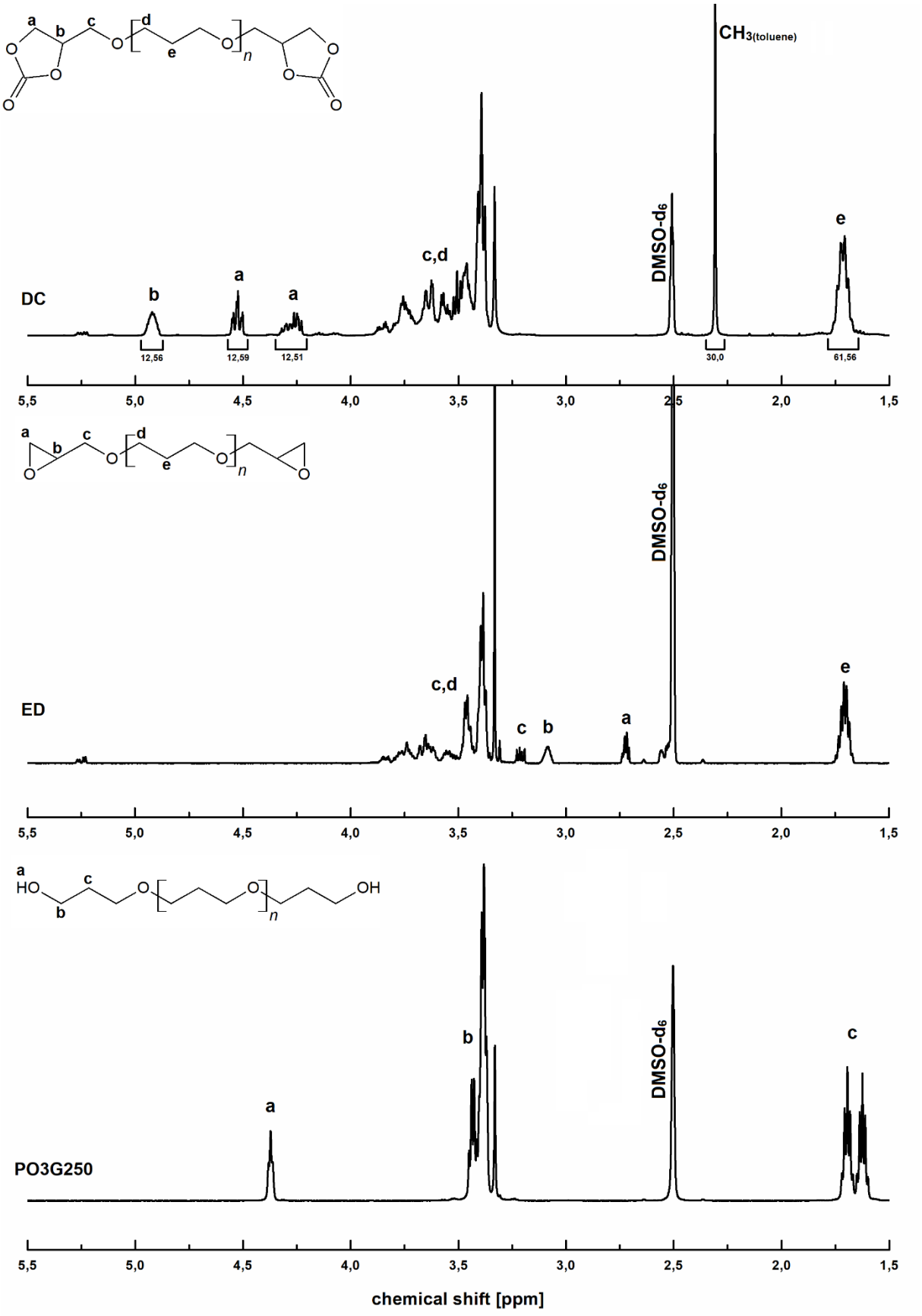

Figure 7 ^{1}H NMR spectra of bio-based polyol and diglycidyl ether as well as bis(cyclic carbonate) with standard solution (THF) in DMSO-d_6

The chemical structure of obtained diglycidyl ether and bis(cyclic carbonate) was also confirmed by ^{1}H NMR, as presented in **Figure 7**. In our previous work, the structure of these semi-products was also confirmed by ^{13}C NMR spectroscopy [21]. The conversion of the hydroxyl group (derived from polyether polyol) into epoxy functional moieties was affirmed. The presence of the characteristic signals of protons attributed to epoxy rings at 3.21 ppm, 3.08 ppm, 2.72 ppm and 2.55 ppm are observed. These typical signals disappeared almost completely in the bis(cyclic carbonate) spectra. New signals associated with the formation of cyclic carbonate functional groups appeared at 4.92 ppm, 4.52 ppm and 4.26 ppm. The peaks located in the range between 3.89 to 3.30 ppm but also at 1.70 ppm have been assigned to the protons in the macromolecular polyol chain. The signal corresponds to the deuterated DMSO solvent is located at 2.50 ppm and the sharp peak at 3.33 ppm is attributable to water. The signal corresponding to protons of the hydroxyl group is noticeable at 5.25 ppm. This suggests the formation of side-products during the first step of the reaction, which is a common phenomenon in this type of chemical reaction [24]. Moreover, the relationship of protons with protons connected to the chlorine atom was also confirmed. The competitive reaction between hydroxyl groups and formed chlorohydrin ether was occurred.

According to ^{1}H NMR spectra, the carbonate equivalent weight (CEW) was determined. The CEW indicates the amount of substance containing one gram-equivalent of functional carbonate [27,28]. CEW for obtained bis(cyclic carbonate) equals 292 g/eq and on this basis it can be estimated that the molar mass of this compound is 584 g/mol (2 eq.).

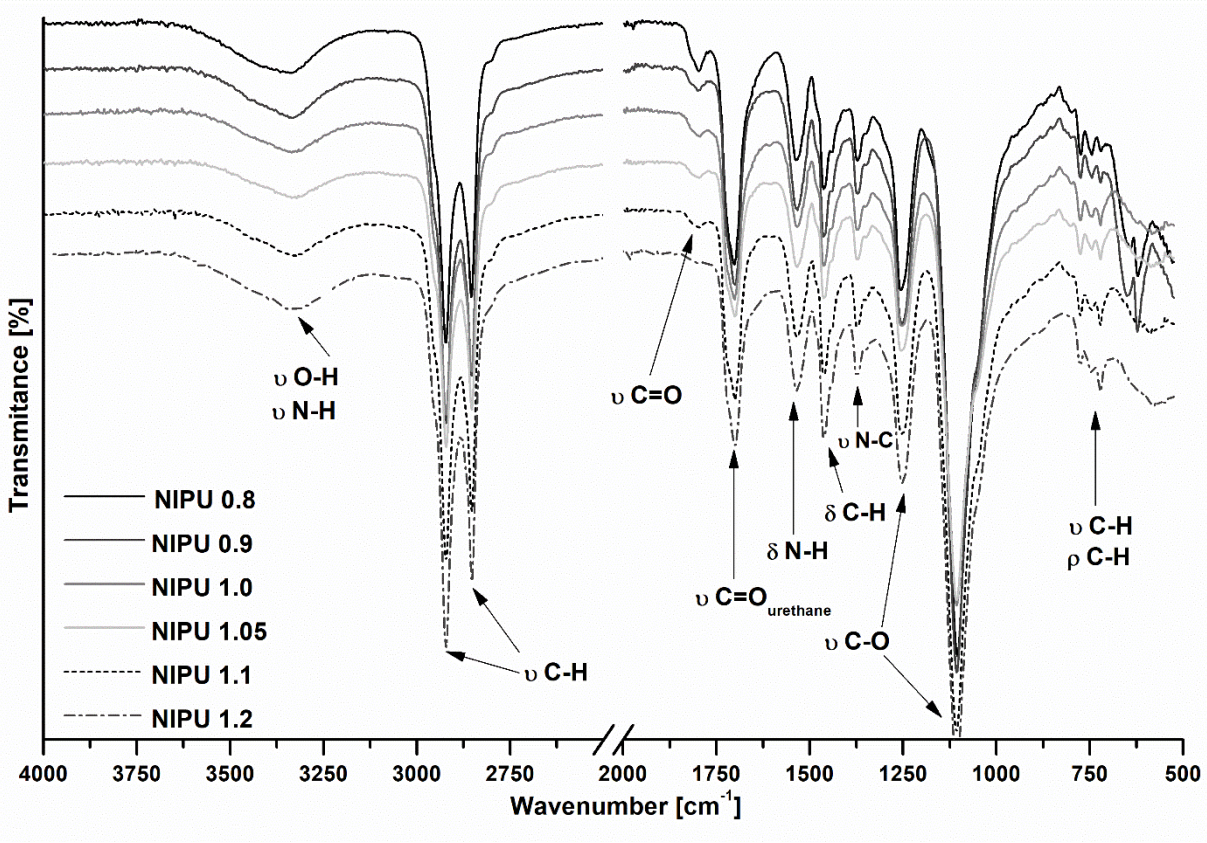

Figure 8 FTIR spectra of the prepared NIPUs

Poly(hydroxy urethane)s (PHUs) were synthesized in the melt via polyaddition of bifunctional five-membered cyclic carbonate (DC) with different amine derivatives of dimerized fatty acids (Priamine). The reaction was performed at mild temperature without using catalyst. Three different approaches to NIPUs synthesis have been used in this paper. The syntheses were carried out for different molar ratios of DC and Priamine 1071 (see **Table 2**). Four different Priamine products were compared, and chemical structures, as well as selected properties of crosslinked materials at four different temperatures (100, 110, 120 and 130°C), were collated.

The synthesized materials exhibited typical infrared characteristics of PUs. The FTIR spectra presented in **Figure 8** and **Figure 9** showed typical vibration and their intensity for characteristic groups in the chemical structure of all obtained materials. The characteristic stretching vibration of hydroxyl (O-H) and amine (N-H) groups in the 3110-3650 cm^{-1} range was observed in all types of samples. In the case of PUs synthesized at molar ratios of DC and Priamine 1071 equal from 0.8 to 1.1, the bands related to carbonyl groups in cyclic carbonate moieties (at 1800 cm^{-1}) are observed (see **Figure 8**). This fact indicates that under applied

conditions the reaction between cyclic carbonate groups and primary amine groups was not completed. The peak in the range between 1660 to 1800 cm^{-1} marks the presence of stretching vibration of hydrogen-bonded carbonyl groups (C=O), which is associated with the presence of urethane groups. Generally, three bands corresponding to the stretching vibrations of carbonyl can be observed in the PUs structure. The first one observed in the range of 1714-1718 cm^{-1} corresponding to the hydrogen-bonded carbonyl vibrations in the less ordered amorphous regions, hydrogen-bonded carbonyl groups in ordered crystalline regions appears at 1685-1706 cm^{-1}, and the last one corresponding to free carbonyl groups displays at around 1730 cm^{-1} [25]. Additional information about the deconvolution process of the carbonyl region of obtained NIPUs are specified below in this subsection. The strong peaks visible in the region from 2700 to 3050 cm^{-1} respectively correspond to the symmetric (at 2854 cm^{-1}) and asymmetric (at 2916 cm^{-1}) stretching vibrations of methylene units (C-H). The absorption intensity of these bands has resulted from a high amount of CH_2 and CH units in the chemical structure of polyether polyol as well as the backbone of used amine. The absorption peak at 1457 cm^{-1} is attributable to the deformation vibrations of the C-H groups. The band observed at 1533 cm^{-1} is related to the out-of-plane bending of N-H groups. Moreover, the peak at 1368 cm^{-1} is assigned to stretching vibration of C-N bonds of the urethane group. The characteristic asymmetric stretch of N-CO-O and stretching C-O-C of urethane groups are observed at about 1250 cm^{-1}. Nanclares et al. [31] reported that this peak increases with the increase of the hard segment content, which is associated with increasing hydrogen bonding interaction between C-O of ether and N-H groups (hard and soft segments interaction). The strong absorption band at 1099 cm^{-1} is related to the vibrations of free ether bonds (C-O-C) of bio-based polyether polyol.

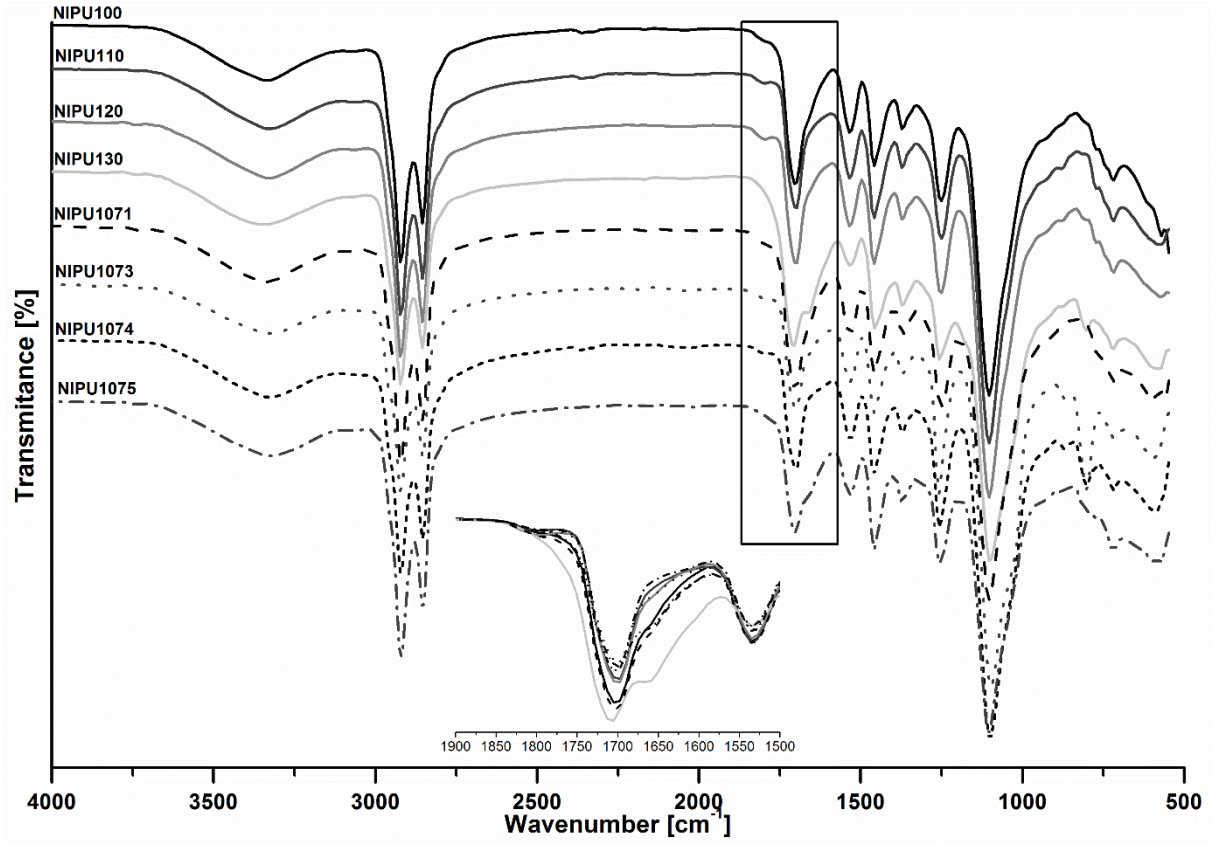

Figure 9 FTIR spectra of the prepared NIPUs (**Appendix S2**- color version of Figure 9)

FTIR spectra were analyzed in the 1600- 1850 cm^{-1} carbonyl stretching region by deconvolution of the carbonyl peaks by using Origin software, as shown in **Table 3**. The area under the C=O peaks was compared with the total area under the evaluated absorbance peak. Three regions have been identified (see **Figure 10**) in which absorption bands occur: 1622- 1662 cm^{-1}, 1705- 1714 cm^{-1} and 1796- 1804 cm^{-1} for hydrogen bonded carbonyl groups, free (non-hydrogen bonded) carbonyl groups and carbonyl groups derived from cyclic carbonate functional groups, respectively. It was observed that with increasing [amine]/[cyclic carbonate] molar ratio during the reaction, the fraction of hydrogen-bonded C=O groups increased and is an amount equal to 24.27% and 64.19% for NIPU0.8 and NIPU1.2, respectively. The same tendency can be observed in the case of rising curing and seasoning temperature. For NIPU100, the lowest fraction (42.52%) of hydrogen bonded carbonyl groups was observed as opposed to the NIPU130 sample (76.88%). A change of the temperature and substrates molar ratio resulted in degree of conversion of cyclic carbonates compounds. At the same time, it was observed that materials prepared in a molar ratio of 1.2 and those prepared from Priamine 1071 showed the lowest amount of free carbonyl groups derived from cyclic carbonate functional groups. This confirms the highest degree of substrates conversion during

the polyaddition of cyclic carbonate with diamine derivatives of dimerized fatty acids. According to the literature, hydrogen bonds cause physical cross-linking and strengthening of materials [32]. In addition, it was found that these data well correlated with results obtained during TGA analysis. It is worth noting that the materials NIPU0.8, NIPU100, and NIPU1073 possess the highest total share of carbonyl groups derived from the urethane groups and cyclic carbonate functional groups.

Table 3 Analysis of the carbonyl region for all prepared samples by the deconvolution of absorption bands (-C=O band in the FTIR spectra).

	-C=O band					
	Peak I: free -C=O		**Peak II: H-bonded -C=O**		**Peak III: -C=O from cyclic carbonate group**	
Material	**Location [cm^{-1}]**	**Fraction [%]**	**Location [cm^{-1}]**	**Fraction [%]**	**Location [cm^{-1}]**	**Fraction [%]**
NIPU0.8	1708.2	64	1663.0	24	1800.3	12
NIPU0.9	1707.1	58	1651.3	34	1804.1	8
NIPU1.0	1706.7	48	1633.1	45	1797.9	7
NIPU1.05	1706.2	44	1631.1	51	1800.5	5
NIPU1.1	1706.0	37	1632.0	60	1797.5	3
NIPU1.2	1705.7	34	1640.9	64	1796.2	2
NIPU100	1706.8	49	1654.4	42	1799.5	9
NIPU110	1705.7	34	1640.9	64	1796.2	2
NIPU120	1705.4	31	1644.5	68	1799.7	1
NIPU130	1714.9	23	1663.8	77	-	0
NIPU1071	1705.7	34	1640.9	64	1796.2	2
NIPU1073	1705.7	45	1642.7	52	1799.4	3
NIPU1074	1706.1	43	1632.3	53	1797.2	4
NIPU1075	1708.3	38	1657.9	58	1801.6	4

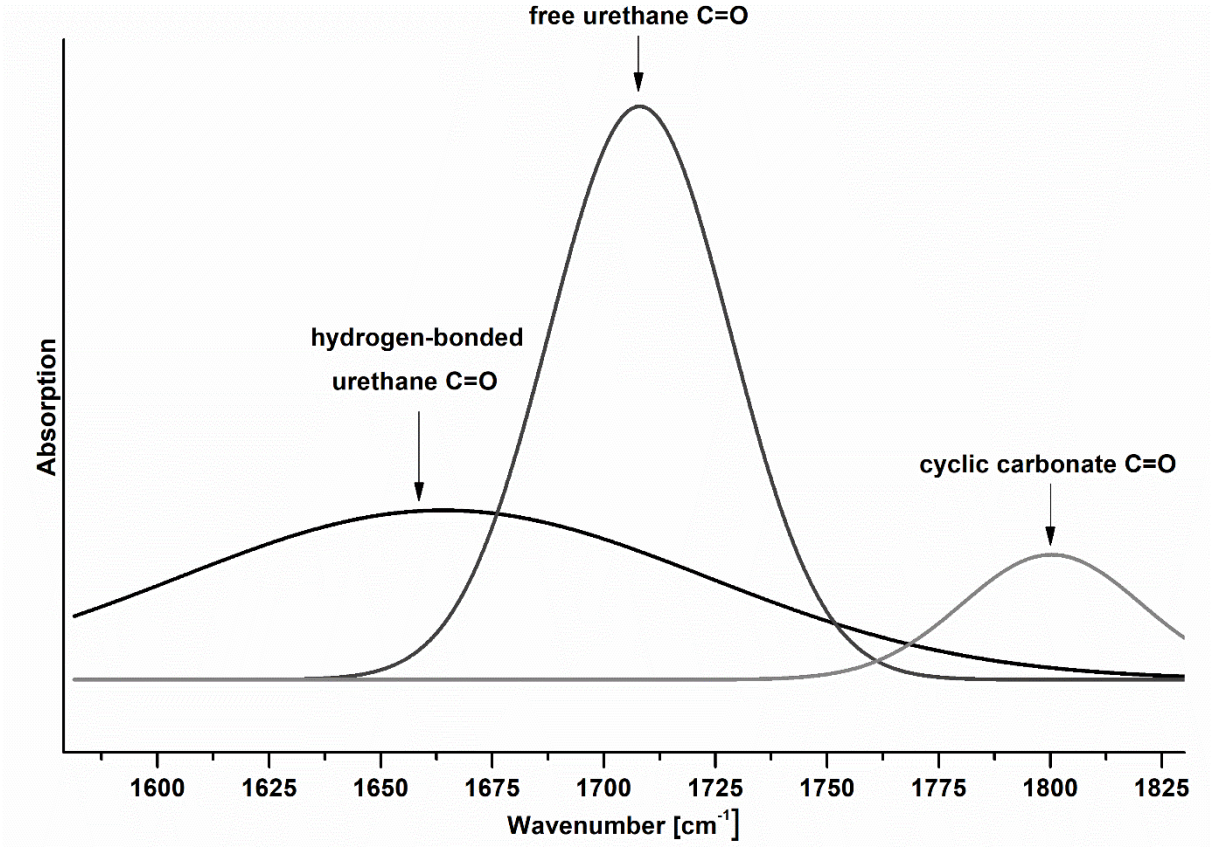

Figure 10 Schematic representation of the deconvolution process of multiplet band attributed to carbonyl groups in the obtained samples

Differential scanning calorimetry measurements

Differential scanning calorimetry (DSC measurements) was used to determine the glass transition temperature (T_g) of the prepared materials. Two dynamic temperature ramps were performed between -80 and 270 ^oC at 20 ^oC min^{-1} under a continuous nitrogen atmosphere (N_2). Typical DSC thermograms from second cycle are given in **Figure 11**. Within the prepared NIPU materials, the T_g was detectable by DSC. In all cases, T_g was very close to each other and existed within the range -34.4 to -29.0 ^oC. It can be seen that there was only one T_g in every curve, indicating that synthesized materials were a homogeneous phase system and the structure was typical for amorphous material. T_g below zero could be ascribed to the presence of long and flexible aliphatic chains introduced to the structure of NIPU by dimer fatty acid-based diamines. The presence of flexible long-chain diamines affects the mobility of polymer chains [33]. On the other hand, the crosslinking degree directly influences the value of T_g, as reported in the literature [34]. Trimer content in the chemical structure of used diamine derivative of dimerized fatty acids (especially Priamine 1071) could have an impact on crosslinking and consequently higher T_g. We also suspect that there could be apparent crosslinking due to

hydrogen bonding. The slight increase of T_g with increasing curing temperature has been also observed. DSC curves of the selected sample (1st, 2nd heating and cooling) are included in the supplementary material (see **Appendix S3**) attached to the present manuscript. No additional exothermic or endothermic transitions are visible on the 1st heating curve, which proves that the materials do not polymerize during the measurement.

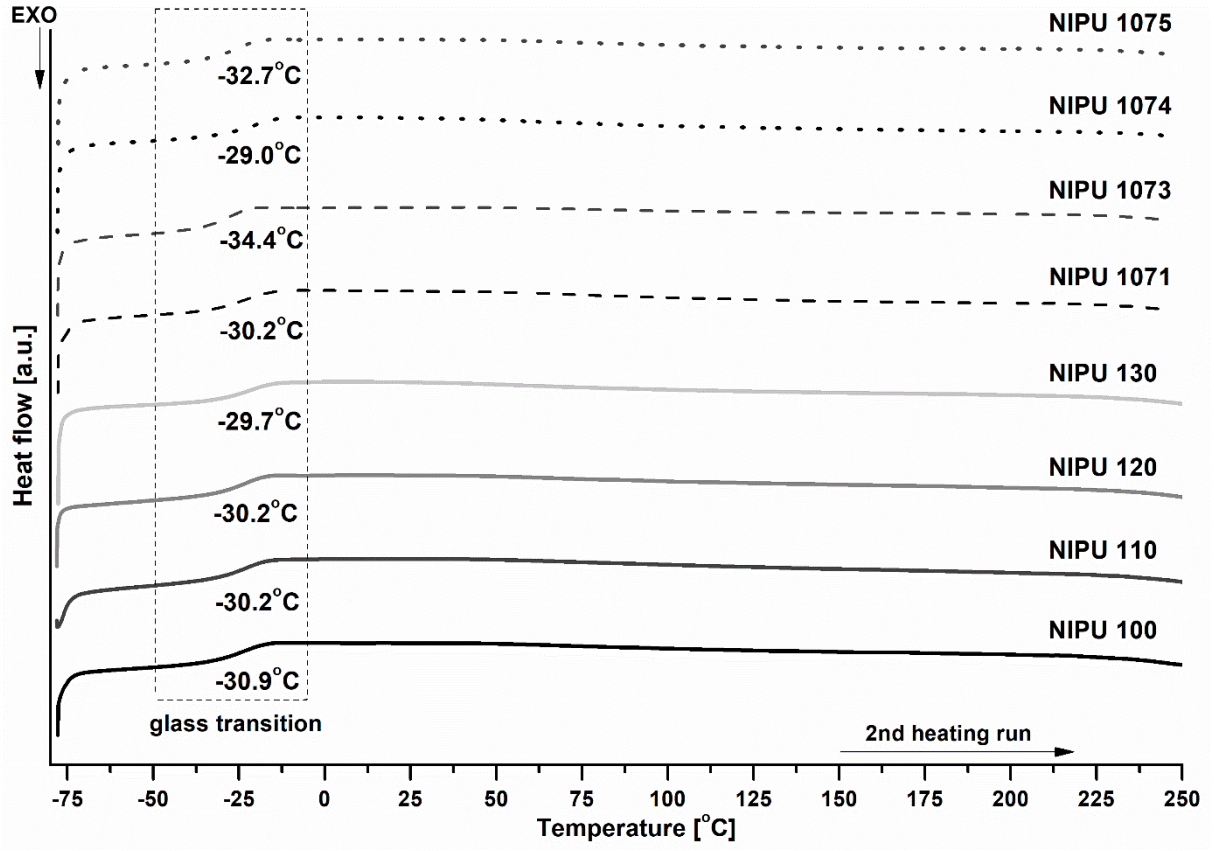

Figure 11 Differential scanning calorimetry (DSC) thermograms of the prepared samples

Thermogravimetric analysis

The TGA was also used to assess the thermal stability of the prepared NIPUs under nitrogen (N_2) atmosphere on the temperature range between room temperature (ca. 25°C) and 600°C. The corresponding results were presented in **Table 4**, **Figure 12** and **Figure 13**. As reported in the scientific literature, the thermal decomposition of urethane linkage may be mediated through three basic mechanisms [35]. In the first case, the urethane bond dissociates into isocyanate and alcohol (starting components). Moreover, by breaking the urethane bond and forming the primary amines, olefins and carbon dioxide. Splitting the urethane bond into carbon dioxide and secondary amines shall also be possible. Both of stages characteristic for NIPUs are also observed for traditional PUs including isocyanate. It can be concluded that all kinds of

PUs materials follow the same pattern of thermal degradation [36,37]. It is worth mentioning that the formation of isocyanate groups during the thermal decomposition of NIPUs is not reported in the literature. In general, isocyanate-based PUs demonstrate a slightly higher thermal stability than NIPUs, but this has not been proven in every job [38]. This is due to the weakening of the bond between oxygen and carbonyl carbon in urethane group under the influence of hydroxyl groups [39].

Based on the DTG curves, the general thermal trend seems to be a double weight loss. Moreover, small peaks are recognized in addition to the main two significant peaks. The initial decomposition temperatures (associated with 5% of weight loss) for prepared samples were roughly between 278 and 290^{o}C, proving that materials had good thermal stability. Subsequently, rapid degradation occurs between 300 and 433^{o}C. This step corresponds to roughly 50% material degradation. The first main step of degradation is attributed to the thermal degradation of urethane bonds to form ammonia, carbon dioxide, and carbon oxide and is a result of -C-N bond low breaking energy [37]. The next step is associated with degradation of ether bonds and aliphatic hydrocarbon chains [40]. The stage associated with 90% of weight loss occurs between 453 and 476^{o}C, respectively. From the data presented in **Table 4**, even though synthesized NIPUs have an aliphatic structure, the char yield at 600 °C has not reached 0%. The occurred residue may be due to small amount of aromatic parts from amine compounds in the chemical structure of products or slow thermal degradation after the main degradation stage [37]. It has been found that the materials with the highest proportion of hydrogen bonds in the chemical structure have the best thermal stability, as these bonds cause internal strengthening of the polymer network. In addition, materials with the largest proportion of free carbonate groups undergo the thermal decomposition process at a lower temperature. As a result, it is enough to provide the lowest energy required for thermal decomposition of the fragment with the lowest thermal stability to start the thermal decomposition process of the obtained material. These results are closely correlated with FTIR analysis.

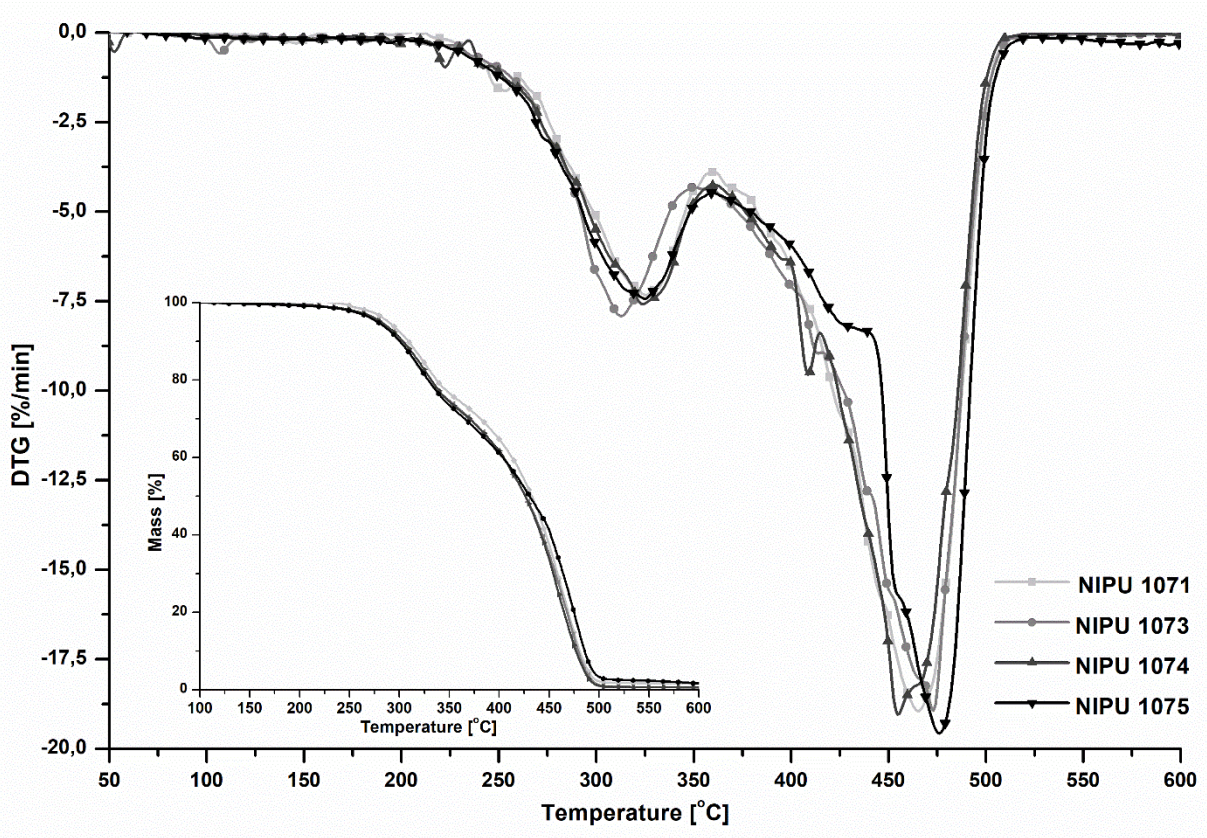

Figure 12 Thermogravimetry (TG) and derivative thermogravimetry (DTG) curves of the NIPUs synthesized using different diamine derivatives of dimerized fatty acids (Priamine®) (**Appendix S4**- color version of Figure 12)

Table 4 Thermal stability of the prepared NIPUs

Material	$T_{5\%}$[°C]	$T_{10\%}$[°C]	$T_{50\%}$[°C]	$T_{90\%}$[°C]	T_{max}[°C] [1st/2nd step]	Residual mass at 600 °C [%]
NIPU 1071	290	308	431	465	318/464	2.6
NIPU 1073	282	302	426	473	313/473	0.6
NIPU 1074	282	304	426	455	324/455	0.6
NIPU 1075	278	300	430	476	325/476	1.6
NIPU 100	283	303	432	453	323/464	1.9
NIPU 110	290	308	431	465	318/464	2.6
NIPU 120	289	309	433	465	326/465	1.7
NIPU 130	288	307	433	470	325/470	3.2

$T_{5\%}$, $T_{10\%}$, $T_{50\%}$, and $T_{90\%}$ is a temperature of 5, 10, 50 and 90% of weight loss, respectively; T_{max} is a temperature of the maximum rate of weight loss during the first and second step

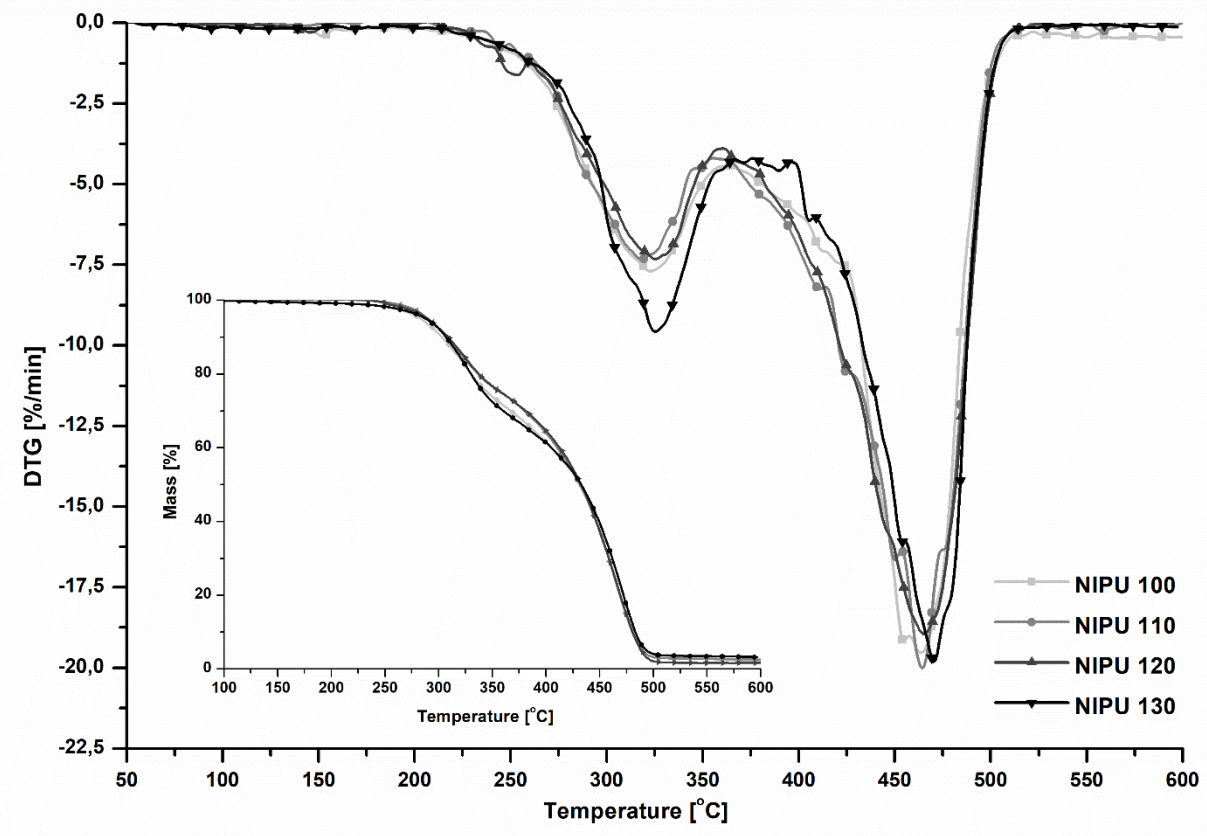

Figure 13 Thermogravimetry (TG) and derivative thermogravimetry (DTG) curves of the NIPUs curing in different temperatures (100, 110, 120 and 130 ^{o}C) (**Appendix S5**- color version of Figure 13)

Swelling index and gel content

Table 5 Swelling properties of NIPUs

Material	Swelling index [%]	Gel content [%]
NIPU 1071	304	92
NIPU 1073	444	87
NIPU 1074	394	89
NIPU 1075	334	91
NIPU 100	341	87
NIPU 110	304	92
NIPU 120	302	91
NIPU 0.9	892 ▲	63 ▼
NIPU 1.0	570	70
NIPU 1.05	438	78
NIPU 1.1	436	86
NIPU 1.2	304	92

With the aim of demonstrating swelling properties of prepared NIPUs, the results of equilibrium swelling in THF are presented in **Table 5**. It is necessary to mention that none of the samples were dissolved in THF during measurements, but NIPU130 has been disintegration into small parts. The swelling index and gel content measurements are able to demonstrate the full conversion of reaction as well as the absence of residual substrates. According to available literature, the lowest swelling index (SI) and the highest gel content (GC) correspond to the maximum crosslinking of material [39]. In the case of our results, the lowest SI and the highest GC possess NIPU1071, which may be related to the content of trimer in the structure of dimer fatty acid-based diamine (Priamine 1071). The content of trimers affects the degree of crosslinking, and hence the distance between crosslinking nodes. The greater the distance between the nodes, the better the solvent penetrates into the structure of the material, which leads to an increase in SI. All the obtained materials are characterized by a high GC (above 87%), which confirms the quantitative conversion of polymerization and the lack of residual monomers. Furthermore, the lower mobility of the polymer chains affects the smaller amount of solvent that can penetrate into the polymer network [41]. The influence of urethane groups in the NIPU chemical structure on interaction with solvent is also important. Urethane groups have the potential to form hydrogen bonding with organic solvent molecules, which facilitates the solvent diffusion and swelling of the sample [42]. According to the deconvolution of the

carbonyl stretching region (C=O) of the obtained NIPUs, it can be seen that the largest amount of free carbonyl groups occurs in the case of sample NIPU0.9 (58%), NIPU100 (49%) as well as NIPU1073 (45%). This sample has more ability for swelling. With the increase in the share of hydrogen bonds between urethane groups, the material's ability to swell processes decreases.

Determination of water absorption

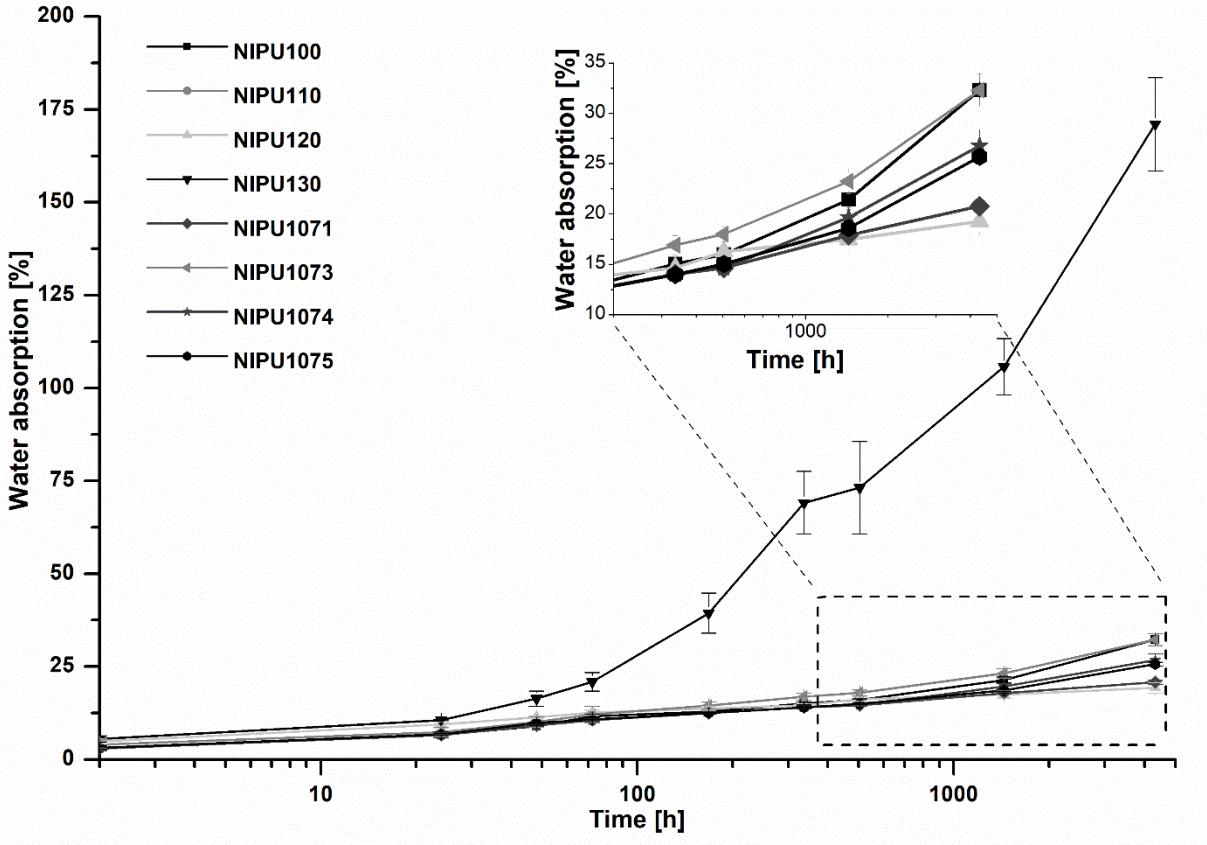

Figure 14 Effect of time immersing in water to the swelling ratio of prepared samples (**Appendix S6**- color version of Figure 14)

Figure 14 demonstrates the changes in weight of prepared samples immersed in distilled water as a function of time. The experiment was carried out for 6 months at room temperature. The higher temperature (130^{o}C) of curing and seasoning affected to degradation of the chemical structure of polymers. As reported in the literature, a high crosslinking density could hinder water molecules to pass through the polymer network structure [34]. The higher the curing and seasoning temperature, the higher the crosslink density and the lower length of macromolecule chains. The lowest water absorption was observed in the case of samples cured at 120^{o}C. The increase in mass as a function of time for materials NIPU100, NIPU110 as well as NIPU120 is not sharp. After about 100 hours, only NIPU130 shows a rapid increase in water penetration

into the polymer structure. Completely different behavior of this sample was observed both during the test in water and also during measurements in THF. The study confirmed earlier assumptions, that at 130^{o}C may occur degradation of macromolecule chains. On the other hand, a high temperature of synthesis (above 120^{o}C) can lead to side reactions and the formation of undesirable side products, such as amidifaction and formation of ureas [2,9,43]. Realized measurements confirmed that this temperature is not suitable for the synthesis of this type of PUs material. After drying, the sample weight decreased <3% relative to the original weight for NIPU cured at 100 ^{o}C (1.9 ± 0.4%), 110 ^{o}C (2.1 ± 0.1%) and 120 ^{o}C (2.7 ± 0.2%). For NIPU130 samples, a 6.9 ± 0.4% weight loss is probably associated with the leaching out of molecules derived from polymer chain degradation. Regarding the use of different diamine derivative of dimerized fatty acids, the results correlate with the obtained crosslinking densities. According to swelling index and gel content measurements, higher crosslinking density occurs for NIPU1071 and NIPU1075. Hence water penetration into the polymer network is limited. The lower mobility of the polymer chains also affects the smaller amount of solvent that can penetrate into the polymer network. The influence of urethane groups in the NIPU chemical structure on interaction with solvent is also important. Urethane groups have the potential to form hydrogen bonding with solvent molecules, which facilitates the solvent diffusion and swelling of the sample [42]. According to the deconvolution of the carbonyl stretching region (C=O) of the obtained NIPUs, it can be seen that the largest amount of free carbonyl groups occurs in the case of sample NIPU100 as well as NIPU1073. These samples have more ability for swelling because they have a greater capacity for forming hydrogen bonding with water molecules [44]. With the increase in the share of hydrogen bonds between urethane groups, the material's ability to swell processes decreases.

Conclusions

The proper selection of reaction conditions, especially [amine]/[cyclic carbonate] molar ratio and appropriate curing temperature, allowed for the successful production of a series of environmentally friendly NIPUs via a three-step method. The type of used diamine derivative of dimerized fatty acids had also a great role in the chemical structure and selected properties of obtained NIPUs. The first step involved the synthesis of diglycidyl ether from bio-based polyether polyol. Next, the cycloaddition of carbon dioxide (CO_2) into epoxy moieties was realized. This process did not require the use of elevated pressure and toxic organic solvents. In the final step, the polyaddition of obtained cyclic carbonate with selected diamine derivative of dimerized fatty acids was fulfilled. On the basis of Gaussian deconvolution of the carbonyl

region (-C=O) found that the correlation between the number of hydrogen bonds and thermal properties as well as susceptibility to swelling has existed. Satisfying thermal properties of the prepared products were demonstrated. The initial decomposition temperatures for obtained materials were roughly between 278 and 290ºC, proving that materials had good thermal stability. Within the prepared NIPU materials, the T_g detectable by DSC existed in the range from -34.4 to -29.0ºC, respectively. We have also shown that hydrogen bonds strengthen PUs materials. It has been shown that the lowest amount of free carbonate groups from cyclic carbonates should be aimed, as their presence reduces the stability of the material. On the basis of obtained results, it was found that the best properties possess materials obtained using 110ºC as a curing temperature. In addition, the [amine]/[cyclic carbonate] molar ratio should be 1.2 to achieve a high degree of substrates conversion. A series of diamine derivatives of dimerized fatty acids produce by Croda company have been used successfully in the synthesis of NIPUs via the proposed method. The presented strategy encompasses several green chemistry principles: using renewable feedstocks, less hazardous syntheses and avoiding toxic organic solvents. To conclude, the obtained NIPUs provide a good potential alternative for traditional PUs materials.

Conflicts of interest

The authors declare that they have no conflict of interest.

Funding

This work was supported by the National Science Centre, Poland [grant number 2018/29/N/ST8/02444]. Author of grant is MSc Eng. Kamila Błażek.

Acknowlegments

The authors wish to thank Allessa (Germany) for kindly providing bio-based polytrimethylene polyol (Sensatis® H250) samples. The authors are also grateful to Croda International (Netherlands) for supplying diamine derivative of dimerized fatty acids (Priamine®) samples used in this study.

We would like to express our gratitude do Professor Maria Filomena Barreiro and her research team from Laboratory of Separation and Reaction Engineering, Associate Laboratory LSRE/LCM, Polytechnic Institute of Bragança, Portugal and MSc Eng. Łukasz Gryglicki for carrying out the TGA analysis. The authors would like to thank PhD Paulina Kosmela from Gdansk University of Technology, Faculty of Chemistry, Department of Polymers Technology, Poland for the DSC measurements. We would like to express our sincere thanks for PhD

Paweł Sowiński from Gdansk University of Technology, Faculty of Chemistry, Nuclear Magnetic Resonance Laboratory for determining chemical structure of our products using NMR spectroscopy.

References

[1] J. Datta, P. Kasprzyk, Thermoplastic Polyurethanes Derived From Petrochemical or Renewable Resources: A Comprehensive Review, Polym. Eng. Sci. 58 (2017) E14–E35. doi:10.1002/pen.

[2] A. Cornille, R. Auvergne, O. Figovsky, B. Boutevin, S. Caillol, A perspective approach to sustainable routes for non-isocyanate polyurethanes, Eur. Polym. J. 87 (2017) 535–552. doi:10.1016/j.eurpolymj.2016.11.027.

[3] P. Wang, S. Liu, Y. Deng, Important Green Chemistry and Catalysis: Non-phosgene Syntheses of Isocyanates – Thermal Cracking Way, Chinese J. Chem. 35 (2017) 821–835. doi:10.1002/cjoc.201600745.

[4] K. Błażek, J. Datta, Renewable natural resources as green alternative substrates to obtain bio-based non-isocyanate polyurethanes-review, Crit. Rev. Environ. Sci. Technol. 49 (2019) 173–211. doi:10.1080/10643389.2018.1537741.

[5] H. Blattmann, M. Fleischer, M. Bähr, R. Mülhaupt, Isocyanate- and Phosgene-Free Routes to Polyfunctional Cyclic Carbonates and Green Polyurethanes by Fixation of Carbon Dioxide, Macromol. Rapid Commun. 35 (2014) 1238–1254. doi:10.1002/marc.201400209.

[6] J. Datta, M. Włoch, Progress in non-isocyanate polyurethanes synthesized from cyclic carbonate intermediates and di- or polyamines in the context of structure–properties relationship and from an environmental point of view, Polym. Bull. 73 (2016) 1459–1496. doi:10.1007/s00289-015-1546-6.

[7] P. Parcheta, J. Datta, Environmental impact and industrial development of biorenewable resources for polyurethanes, Crit. Rev. Environ. Sci. Technol. 47 (2017) 1986–2016. doi:10.1080/10643389.2017.1400861.

[8] A. Ekman, M. Campos, S. Lindahl, M. Co, P. Börjesson, E.N. Karlsson, C. Turner, Bioresource utilisation by sustainable technologies in new value-added biorefinery concepts - Two case studies from food and forest industry, J. Clean. Prod. 57 (2013) 46–58. doi:10.1016/j.jclepro.2013.06.003.

[9] C. Carre, Y. Ecochard, S. Caillol, L. Averous, From the Synthesis of Biobased Cyclic Carbonate to Polyhydroxyurethanes : A Promising Route towards Renewable Non-Isocyanate Polyurethanes, ChemSusChem. 12 (2019) 1–22. doi:10.1002/cssc.201900737.

[10] M. Bähr, R. Mülhaupt, Linseed and soybean oil-based polyurethanes prepared via the non-isocyanate route and catalytic carbon dioxide conversion, Green Chem. 14 (2012) 483–489. doi:10.1039/c2gc16230j.

[11] V. Besse, R. Auvergne, S. Carlotti, G. Boutevin, B. Otazaghine, S. Caillol, J.P. Pascault, B. Boutevin, Synthesis of isosorbide based polyurethanes: An isocyanate free method, React. Funct. Polym. 73 (2013) 588–594. doi:10.1016/j.reactfunctpolym.2013.01.002.

[12] S. Schmidt, N.E. Göppert, B. Bruchmann, R. Mülhaupt, Liquid sorbitol ether carbonate as intermediate for rigid and segmented non-isocyanate polyhydroxyurethane thermosets, Eur. Polym. J. 94 (2017) 136–142. doi:10.1016/j.eurpolymj.2017.06.043.

[13] M. Fleischer, H. Blattmann, R. Mülhaupt, Glycerol-, pentaerythritol- and trimethylolpropane-based polyurethanes and their cellulose carbonate composites prepared via the non-isocyanate route with catalytic carbon dioxide fixation, Green Chem. 15 (2013) 934–942. doi:10.1039/c3gc00078h.

[14] Q. Chen, K. Gao, C. Peng, H. Xie, Z.K. Zhao, M. Bao, Preparation of lignin/glycerol-based bis(cyclic carbonate) for the synthesis of polyurethanes, Green Chem. 17 (2015) 4546–4551. doi:10.1039/c5gc01340b.

[15] N. Esmaeili, M.J. Zohuriaan-Mehr, A. Salimi, M. Vafayan, Tannic acid derived non-isocyanate polyurethane networks: Synthesis, curing kinetics, antioxidizing activity and cell viability, Thermochim. Acta. 664 (2018) 64–72. doi:10.1016/j.tca.2018.04.013.

[16] M. Fache, E. Darroman, V. Besse, R. Auvergne, S. Caillol, B. Boutevin, Vanillin, a promising biobased building-block for monomer synthesis, Green Chem. 16 (2014) 1987–1998. doi:10.1039/C3GC42613K.

[17] M. Kathalewar, A. Sabnis, D. D'Mello, Isocyanate free polyurethanes from new CNSL based bis-cyclic carbonate and its application in coatings, Eur. Polym. J. 57 (2014) 99–108. doi:10.1016/j.eurpolymj.2014.05.008.

[18] M. Bähr, A. Bitto, R. Mülhaupt, Cyclic limonene dicarbonate as a new monomer for non-isocyanate oligo- and polyurethanes (NIPU) based upon terpenes, Green Chem. 14 (2012) 1447–1454. doi:10.1039/c2gc35099h.

[19] M. Włoch, J. Datta, K. Błażek, The Effect of High Molecular Weight Bio-based Diamine Derivative of Dimerized Fatty Acids Obtained from Vegetable Oils on the Structure, Morphology and Selected Properties of Poly(ether-urethane-urea)s, J. Polym. Environ. (n.d.) 1–13. doi:10.1007/s10924-017-1059-5.

[20] M. Włoch, J. Datta, Synthesis, Structure and Properties of Poly(ester-Urethane-Urea)s Synthesized Using Biobased Diamine, J. Renew. Mater. 4 (2016) 72–77. doi:10.7569/JRM.2015.634130.

[21] K. Błażek, J. Datta, A. Cichoracka, Sustainable synthesis of cyclic carbonates from bio-based polyether polyol: the structure characterization, rheological behaviour and thermal properties, Polym. Int. 68 (2019) 1968–1979. doi:10.1002/pi.5908.

[22] M. El Fray, J. Skrobot, D. Bolikal, J. Kohn, Synthesis and characterization of telechelic macromers containing fatty acid derivatives, React. Funct. Polym. 72 (2012) 781–790. doi:10.1016/j.reactfunctpolym.2012.07.010.

[23] C. Carré, L. Bonnet, L. Avérous, Solvent- and catalyst-free synthesis of fully biobased nonisocyanate polyurethanes with different macromolecular architectures, RSC Adv. 5 (2015) 100390–100400. doi:10.1039/c5ra17638g.

[24] H. Kang, M. Lee, J. Yoon, M. Yoon, Improvement of the Phase-Transfer Catalysis Method for Synthesis of Glycidyl Ether, J. Am. Oil Chem. Soc. 42 (2000) 423–429.

[25] P. Kasprzyk, J. Datta, Novel bio-based thermoplastic poly(ether-urethane)s. Correlations between the structure, processing and properties, Polymer (Guildf). 160 (2019) 1–10. doi:10.1016/j.polymer.2018.11.032.

[26] P. Kasprzyk, J. Datta, Effect of molar ratio [NCO]/[OH] groups during prepolymer chains extending step on the morphology and selected mechanical properties of final bio-based thermoplastic poly(ether-urethane) materials, Polym. Eng. Sci. 58 (2018) E199–E206. doi:10.1002/pen.24874.

[27] A. Cornille, M. Blain, R. Auvergne, B. Andrioletti, B. Boutevin, S. Caillol, A study of cyclic carbonate aminolysis at room temperature: Effect of cyclic carbonate structures and solvents on polyhydroxyurethane synthesis, Polym. Chem. 8 (2017) 592–604. doi:10.1039/c6py01854h.

[28] A. Cornille, C. Guillet, S. Benyahia, C. Negrell, Room temperature flexible isocyanate-free polyurethane foams, Eur. Polym. J. 84 (2016) 873–888. doi:10.1016/j.eurpolymj.2016.05.032.

[29] N. Kébir, S. Nouigues, P. Moranne, F. Burel, Nonisocyanate thermoplastic polyurethane elastomers based on poly(ethylene glycol) prepared through the transurethanization approach, J. Appl. Polym. Sci. 134 (2017) 1–9. doi:10.1002/app.44991.

[30] H. R, The Pine Biorefinery Platform Chemicals Value Chain, in: A. Pandey, R. Hofer, M. Taherzadeh, K. Madhavan Nampoothiri, C. Larroche (Eds.), Ind. Biorefineries White Biotechnol., Elsevier, 2015: pp. 127–155. doi:10.1016/B978-0-444-63453-5.00004-5.

[31] J. Nanclares, Z.S. Petrovic, I. Javni, M. Ionescu, F. Jaramillo, Segmented polyurethane elastomers by nonisocyanate route, J. Appl. Polym. Sci. 132 (2015) 7–14. doi:10.1002/app.42492.

[32] P. Kasprzyk, E. Sadowska, J. Datta, Investigation of Thermoplastic Polyurethanes Synthesized via Two Different Prepolymers, J. Polym. Environ. (2019). doi:10.1007/s10924-019-01543-7.

[33] X. Sheng, G. Ren, Y. Qin, X. Chen, X. Wang, F. Wang, Quantitative synthesis of bis(cyclic carbonate)s by iron catalyst for non-isocyanate polyurethane synthesis, Green Chem. 17 (2015) 373–379. doi:10.1039/c4gc01294a.

[34] X. He, X. Xu, Q. Wan, G. Bo, Y. Yan, Synthesis and Characterization of Dimmer-Acid-Based Nonisocyanate Polyurethane and Epoxy Resin Composite, Polymers (Basel). 9 (2017) 649. doi:10.3390/polym9120649.

[35] R. Font, A. Fullana, J.A. Caballero, J. Candela, A. Garcı, Pyrolysis study of polyurethane, J. Anal. Appl. Pyrolysis. 59 (2001) 63–77.

[36] I. Javni, Z.S. Petrovic, A. Guo, R. Fuller, Thermal Stability of Polyurethanes Based on Vegetable Oils, J. Appl. Polym. Sci. 77 (1999) 1723–1734.

[37] Z. Karami, K. Kabiri, M.J. Zohuriaan-mehr, Non-isocyanate polyurethane thermoset based on a bio-resourced star- shaped epoxy macromonomer in comparison with a cyclocarbonate fossil- based epoxy resin : A preliminary study on thermo-mechanical and antibacterial properties, J. CO2 Util. 34 (2019) 558–567. doi:10.1016/j.jcou.2019.08.009.

[38] A. Cornille, C. Guillet, S. Benyahya, C. Negrell, B. Boutevin, S. Caillol, Room temperature flexible isocyanate-free polyurethane foams, Eur. Polym. J. 84 (2016) 873–888. doi:10.1016/j.eurpolymj.2016.05.032.

[39] A. Cornille, G. Michaud, F. Simon, S. Fouquay, R. Auvergne, B. Boutevin, S. Caillol, Promising mechanical and adhesive properties of isocyanate-free poly(hydroxyurethane), Eur. Polym. J. 84 (2016) 404–420. doi:10.1016/j.eurpolymj.2016.09.048.

[40] T. Quérette, E. Fleury, N. Sintes-Zydowicz, Non-isocyanate polyurethane nanoparticles prepared by nanoprecipitation, Eur. Polym. J. 114 (2019) 434–445. doi:10.1016/j.eurpolymj.2019.03.006.

[41] P. Jutrzenka Trzebiatowska, A. Santamaria Echart, T. Calvo Correas, A. Eceiza, J. Datta, The changes of crosslink density of polyurethanes synthesised with using recycled component. Chemical structure and mechanical properties investigations, Prog. Org. Coatings. 115 (2018) 41–48. doi:10.1016/j.porgcoat.2017.11.008.

[42] Z. Karami, M.J. Zohuriaan-Mehr, A. Rostami, Bio-based thermo-healable non-isocyanate polyurethane DA network in comparison with its epoxy counterpart, J. CO2 Util. 18 (2017) 294–302. doi:10.1016/j.jcou.2017.02.009.

[43] L. Maisonneuve, E. Rix, E. Grau, H. Cramail, Isocyanate-Free Routes to Polyurethanes and Poly (hydroxy Urethane)s, Chem. Rev. 115 (2015) 12407–12439. doi:10.1021/acs.chemrev.5b00355.

[44] K.L. Mittal, Polyimides and other high-temperature polymers: synthesis, characterization, and applications. Volume 5, 2009.